DTU Library

Eects of additive noise on formation of spatial patterns in an activator-inhibitor system

Tian, Canrong; Ling, Zhi; Zhang, Lai; Pedersen, Michael

[Link back to DTU Orbit](#)

Effects of additive noise on formation of spatial patterns in an activator-inhibitor system

Canrong Tian

School of Mathematical and Physical Sciences, Yancheng Institute of Technology, Yancheng 224003, China

Zhi Ling and Lai Zhang*

School of Mathematical Science, Yangzhou University, Yangzhou 225002, China

Michael Pedersen

Department of Applied Mathematics and Computer Science,
Technical University of Denmark, DK-2800 Kgs. Lyngby, Denmark

We explore the impact of additive noise on the spatial patterns emerging in an activator-inhibitor system, which is modeled by a stochastic reaction-diffusion system. By means of multiscale analysis we derive an amplitude equation around the onset of the Hopf bifurcation. Most importantly, we formulate a threshold value in terms of the noise tensor, which determines whether the additive noise will sustain or destroy the Hopf bifurcation. Finally, we carry out numerical simulations to demonstrate how the additive noise can induce the emergence of spiral and target wave patterns when a Hopf bifurcation occurs.

I. INTRODUCTION

The theory of pattern formation was first proposed by Turing [1] in a reaction-diffusion system. The system consists of two chemical substances, one activator and one inhibitor. When the inhibitor diffuses faster than the activator, there is a possibility that an initial random density distribution of the two species can eventually evolve into a stationary spatially inhomogeneous distribution. Such self-organized spatial patterns are usually called Turing patterns. Turing patterns have been observed to occur in chemical systems via the so-called CIAM reaction models [2–4], and an example of CIAM reaction models proposed by Duffet and Boissonade [5] is as follows

$$
\begin{aligned}
\frac{\partial u}{\partial t} &= \Delta u + u - av + cuv - u^3, \\
\frac{\partial v}{\partial t} &= d\Delta v + u - bv,
\end{aligned}
\tag{1}
$$

where u (activator) and v (inhibitor) are the concentrations of the two chemical substances, respectively. d is the diffusion ratio between the two substances.

During the last few decades, pattern formation has attracted great attention, and a large amount of attention has been paid to the formation of spatial patterns in physically homogeneous systems [6–8]. There are two types of self-organized spatial patterns in reaction-diffusion systems: Turing patterns and spiral wave patterns. The wave pattern is the focus of this work. Spiral waves have been observed in physical [9, 10], chemical [11, 12], and biological [13, 14] systems, where wave propagation is driven by a source of energy stored in the medium. Understanding the mechanisms responsible for such a pattern formation is one of the central problems in nonlinear science. Both the Turing pattern and the spiral wave pattern are spatially regular steady states, which are far from the thermo-dynamic equilibrium. Bifurcation theory plays a central role in understanding the mechanisms of pattern formation. In fact, the spiral wave pattern is a result of a Hopf bifurcation while the Turing pattern is a saddle-node bifurcation.

However, due to widespread environmental noise [15–20], no real-life systems are really physically homogeneous. Therefore understanding how heterogeneous surroundings contribute to the emergence of spatial patterns is of great importance. Unlike bifurcation theory in deterministic systems, in stochastic systems, near a change of stability, the slow modes are often dominant, and therefore there occur a natural separation of timescales. On a long-time scale, the amplitudes of the dominant modes are described by a stochastic ordinary differential equation. Using bifurcation theory, it has been shown that the additive noise can destroy a pitchfork bifurcation [21] or alter a saddle-node bifurcation [22–25]. Moreover, additive noise is shown to play an important role in the formation of spatial patterns in a variety of systems [26–32]. However, there has been no study of the impact of additive noise on a Hopf bifurcation in stochastic partial differential equations, which is the aim of this paper. To this aim, we have updated the system (1) by adding additive noise

$$
\begin{aligned}
\frac{\partial u}{\partial t} &= \Delta u + u - av + cuv - u^3 + \delta\zeta(t), \\
\frac{\partial v}{\partial t} &= d\Delta v + u - bv + \delta\zeta(t),
\end{aligned}
\tag{2}
$$

where the system (2) is subject to a periodic bound-

* Corresponding author: lai.zhang@yzu.edu.cn

ary condition. δ is the noise tensor. $\zeta(t)$ is a Gaussian noise which obeys $\langle\zeta(t)\rangle = 0$ and $\langle\zeta(t)\zeta(\tau)\rangle = 2\delta(t-\tau)$, i.e., $\zeta(t)$ is uncorrelated in time.

The paper is structured as follows. In Section II, we apply multiscale analysis to the stochastic reaction-diffusion system (2). We derive an amplitude equation and find a threshold value in terms of the noise tensor. The threshold determines whether the additive noise will sustain or destroy the Hopf bifurcation that occurs in the deterministic system (1). In Section III, we perform numerical simulations to illustrate our analytical findings and further to show that spiral and target waves emerge in the stochastic system. Our paper closes with a brief conclusion.

II. THE EFFECT OF ADDITIVE NOISE ON A HOPF BIFURCATION

In this section we first explore the conditions for a Hopf bifurcation to occur by analyzing the linear stability of the spatially uniform equilibrium to the system (1), then derive the associated amplitude equation for the emerging oscillatory dynamics. Finally we formulate a threshold value in terms of the noise tensor, which determines the impact of the additive noise on the Hopf bifurcation.

The system (1) has a trivial equilibrium $(u^*, \ v^*) \ = \ (0,0)$, and two positive equilibria $(u_1, \ v_1) \ = \ (\frac{c+\sqrt{c^2+4(b-a)b}}{2b}, \frac{c+\sqrt{c^2+4(b-a)b}}{2b^2})$ and $(u_2, \ v_2) \ = \ (\frac{c-\sqrt{c^2+4(b-a)b}}{2b}, \frac{c-\sqrt{c^2+4(b-a)b}}{2b^2})$. The two positive equilibria exist when $c \geq 2\sqrt{b(a-b)}$. In this paper, we focus on the Hopf bifurcation around the equilibrium (u^*, v^*), and since the study of the Hopf bifurcation around the other two equilibria is technically similar, it is omitted here. For the deterministic system (1), it is easy to see that the Hopf bifurcation around the equilibrium (u^*, v^*) occurs at $b = 1 \equiv b_c$ provided that $a > 1$, and periodic dynamics emerges when $b < b_c$ (Appendix A). We explore in system (2) below, how additive noise affects the oscillatory dynamics.

For the sake of simplicity, we rewrite the system (2) around b_c with $\mathbf{U} = (u, v)^T$ and $\mathbf{U_i} = (u_i, v_i)^T$ as follows

$$\frac{\partial\mathbf{U}}{\partial t} = L\mathbf{U} + (b_c - b)M\mathbf{U}$$
$$+ \frac{1}{2}B(\mathbf{U}, \mathbf{U}) + \frac{1}{6}C(\mathbf{U}, \mathbf{U}, \mathbf{U}) + \delta\zeta(t), \quad (3)$$

where

$$L = \begin{pmatrix} \Delta+1 & -a \\ 1 & d\Delta - b_c \end{pmatrix},$$

$$M = \begin{pmatrix} 0 & 0 \\ 0 & 1 \end{pmatrix},$$

$$B(\mathbf{U_1}, \mathbf{U_2}) = \begin{pmatrix} cu_1v_2 + cu_2v_1 \\ 0 \end{pmatrix},$$

$$C(\mathbf{U_1}, \mathbf{U_2}, \mathbf{U_3}) = \begin{pmatrix} -6u_1u_2u_3 \\ 0 \end{pmatrix}. \quad (4)$$

The solution $\mathbf{U} = (u, v)^T$ can be written as

$$\begin{pmatrix} u \\ v \end{pmatrix} = \sum_k \begin{pmatrix} u^{(k)} \\ v^{(k)} \end{pmatrix} e^{\lambda t}, \quad (5)$$

where λ is the growth rate of the perturbation in time t, and k is the wave number.

Now we carry out a multiscale analysis to derive the amplitude equation of the stochastic partial differential equation (3). Around the Hopf bifurcation point, the dynamics has a fast time scale, $t \sim 2\pi/\omega$ and a fast mode of frequency $\omega = \sqrt{a-1}$ (Appendix). Set $t = \omega T + \varepsilon^2\tau$ such that the variable t depends on the two variables T and τ. Here ε is a control parameter, representing the dimensionless distance to the threshold b_c. T is of the same order as t and is called the fast timescale; τ is high-order infinitesimal with respect to t and is called the slow timescale. The solution of the system (3) is written as a weakly nonlinear expansion around the small control parameter ε. For the multiscale analysis around the onset of the Hopf bifurcation, we set

$$\begin{pmatrix} u \\ v \end{pmatrix} = \varepsilon\begin{pmatrix} u_1 \\ v_1 \end{pmatrix} + \varepsilon^2\begin{pmatrix} u_2 \\ v_2 \end{pmatrix} + \varepsilon^3\begin{pmatrix} u_3 \\ v_3 \end{pmatrix} + O(\varepsilon^4),$$
$$\frac{\partial}{\partial t} = \omega\frac{\partial}{\partial T} + \varepsilon^2\frac{\partial}{\partial\tau}, \quad (6)$$
$$b_c - b = \mu\varepsilon^2,$$
$$\delta = \delta_0\varepsilon^3 + O(\varepsilon^4),$$

where u_j and v_j $(j = 1, 2, 3)$ are functions of T and τ, which correspond to the slow time scale solution when all transients have decayed.

Inserting the expansions (6) into the equation (3) and collecting terms of the the same order in ε, we obtain the following systems

$$O(\varepsilon): \quad (\omega\frac{\partial}{\partial T}\mathbf{I} - L)\begin{pmatrix} u_1 \\ v_1 \end{pmatrix} = 0,$$

$$O(\varepsilon^2): \quad (\omega\frac{\partial}{\partial T}\mathbf{I} - L)\begin{pmatrix} u_2 \\ v_2 \end{pmatrix} = \mathbf{F}, \quad (7)$$

$$O(\varepsilon^3): \quad (\omega\frac{\partial}{\partial T}\mathbf{I} - L)\begin{pmatrix} u_3 \\ v_3 \end{pmatrix} = \mathbf{G},$$

where

$$\mathbf{F} = \frac{1}{2}B(\mathbf{U_1}, \mathbf{U_1}),$$

$$\mathbf{G} = \mu M\mathbf{U_1} - \frac{\partial}{\partial\tau}\mathbf{U_1}$$
$$+ \frac{1}{2}B(\mathbf{U_1}, \mathbf{U_2}) + \frac{1}{2}B(\mathbf{U_2}, \mathbf{U_1}) \quad (8)$$
$$+ \frac{1}{6}C(\mathbf{U_1}, \mathbf{U_1}, \mathbf{U_1}) + \begin{pmatrix} \delta_0 \\ \delta_0 \end{pmatrix}\zeta(T/\omega).$$

Since L is the linear operator from the equation (3) at the onset of the Hopf bifurcation, $(u_1, v_1)^T$ is actually an eigenvector corresponding to the eigenvalue $i\omega$. Therefore, for the $O(\varepsilon)$-system, the solution is given in the form

$$(u_1, v_1)^T = \rho A(\tau)e^{iT} + c.c. \quad (9)$$

with

$$\rho := (\rho_1, \rho_2)^T \in Ker(L - i\omega \mathbf{I}),$$

where $A(\tau)$ is the amplitude of the solution, still arbitrary at this level, and c.c. is the complex conjugate of $\rho A(\tau) e^{iT}$. Noticing that the wavenumber $k_c = 0$ for the Hopf bifurcation, the eigenvector ρ associated with the eigenvalues $i\omega$ is $\rho \cos k_c x \equiv \rho$, where ρ is the kernel of $L_c - i\omega \mathbf{I}$ and

$$L_c = \begin{pmatrix} 1 & -a \\ 1 & -1 \end{pmatrix}. \tag{10}$$

Hence the eigenvector ρ is defined up to a constant and we shall make a normalization in the following way

$$\rho = (\rho_1, 1)^T, \text{ with } \rho_1 = 1 + i\sqrt{a - 1}. \tag{11}$$

Now, we turn to the $O(\varepsilon^2)$-system. Substituting (9) into the system (8) and using $\rho_1 = 1 + i\sqrt{a - 1}$ and $\rho_2 = 1$, we get

$$\mathbf{F} = \begin{pmatrix} c\rho_1 A^2 e^{i2T} + c\bar{\rho}_1 \bar{A}^2 e^{-i2T} \\ 0 \end{pmatrix} + \begin{pmatrix} 2c|A|^2 \\ 0 \end{pmatrix}.$$

Since the right-hand side of above equation does not have resonance (i.e., $\mathbf{F}$ does not have the term e^{iT}), the Fredholm alternative is automatically satisfied. The solution to the second equation of the system (7) is then explicitly computed in terms of the parameters of the full system

$$\begin{pmatrix} u_2 \\ v_2 \end{pmatrix} = |A|^2 \begin{pmatrix} p_0 \\ q_0 \end{pmatrix} + A^2 \begin{pmatrix} p_2 \\ q_2 \end{pmatrix} e^{i2T} + c.c., \tag{12}$$

where $(p_0, q_0)^T$ and $(p_2, q_2)^T$ are, respectively, the solutions of the following two linear systems

$$-L_c \begin{pmatrix} p_0 \\ q_0 \end{pmatrix} = \begin{pmatrix} 2c \\ 0 \end{pmatrix}, \tag{13}$$

$$(2i\omega \mathbf{I} - L_c) \begin{pmatrix} p_2 \\ q_2 \end{pmatrix} = \begin{pmatrix} c\rho_1 \\ 0 \end{pmatrix}. \tag{14}$$

Hence we get

$$p_0 = q_0 = \frac{2c}{a - 1}, \quad p_2 = \frac{c(3 - 2a + 3i\sqrt{a-1})}{3(1 - a)},$$

$$q_2 = \frac{c(1 + i\sqrt{a-1})}{3(1 - a)}. \tag{15}$$

Finally we consider the $O(\varepsilon^3)$-system. According to the Fredholm alternative condition, the vector function of the right-hand side of the third equation in system (7) must be orthogonal to the nontrivial kernel of the operator $(\omega\frac{\partial}{\partial T}\mathbf{I} - L)^*$ in order to ensure the existence of nontrivial solution to this equation, where $(\omega\frac{\partial}{\partial T}\mathbf{I} - L)^*$ is the adjoint operator of $(\omega\frac{\partial}{\partial T}\mathbf{I} - L)$. The nontrivial kernel of the operator $(\omega\frac{\partial}{\partial T}\mathbf{I} - L)^*$ is written as $\rho^* e^{iT}$, where

$$\rho^* e^{iT} \equiv \begin{pmatrix} \rho_1^* \\ \rho_2^* \end{pmatrix} e^{iT} = \begin{pmatrix} 1 \\ -1 - i\sqrt{a-1} \end{pmatrix} e^{iT}. \tag{16}$$

In order to ensure that the Fredholm alternative condition is satisfied, we only consider the resonance of $\mathbf{G}$. The Fredholm alternative condition then dictates that $\langle \rho^* e^{iT}, \mathbf{G} \rangle = 0$, where $\langle a(T), b(T) \rangle = \int_0^{2\pi} \bar{a}(T) b(T) dT$. Then we have

$$\mu A \left(\bar{\rho}_1^*, \bar{\rho}_2^* \right) M \begin{pmatrix} \rho_1 \\ \rho_2 \end{pmatrix} - \frac{\partial A}{\partial \tau} \left(\bar{\rho}_1^*, \bar{\rho}_2^* \right) \begin{pmatrix} \rho_1 \\ \rho_2 \end{pmatrix}$$

$$+ |A|^2 A \left(\bar{\rho}_1^*, \bar{\rho}_2^* \right) \begin{pmatrix} c(\rho_1 q_0 + \bar{\rho}_1 q_2 + \rho_2 p_0 + \bar{\rho}_2 p_2) \\ 0 \end{pmatrix}$$

$$+ |A|^2 A \left(\bar{\rho}_1^*, \bar{\rho}_2^* \right) \begin{pmatrix} -3|\rho_1|^2 \rho_1 \\ 0 \end{pmatrix}$$

$$+ \frac{\delta_0}{2\pi} \left(\bar{\rho}_1^*, \bar{\rho}_2^* \right) \begin{pmatrix} 1 \\ 1 \end{pmatrix} \int_0^{2\pi} \zeta(T/\omega) e^{-iT} dT = 0. \tag{17}$$

Direct calculation yields that

$$\mu A \bar{\rho}_2^* - \frac{\partial A}{\partial \tau}(\rho_1 + \bar{\rho}_2^*)$$

$$+ |A|^2 A \left(-3|\rho_1|^2 \rho_1 + c(\rho_1 q_0 + \bar{\rho}_1 q_2 + \rho_2 p_0 + \bar{\rho}_2 p_2) \right)$$

$$+ \frac{\delta_0}{2\pi}(1 + \bar{\rho}_2^*) \int_0^{2\pi} \zeta(T/\omega) e^{-iT} dT = 0. \tag{18}$$

Multiply Eq. (18) by ε^3 and set the amplitude $\hat{A} = \varepsilon A$. For sake of simplicity, we omit the tildes. By Eq. (6) and Eq. (18), we obtain the amplitude equation

$$\frac{dA}{dt} = (b_c - b)P_1 A - P_3 |A|^2 A$$

$$- \frac{\delta\sqrt{a-1}}{4\pi} \int_0^{2\pi/\omega} \zeta(t) e^{-i\omega t} dt, \tag{19}$$

where

$$P_1 = \frac{1}{2} + \frac{i}{2\sqrt{a-1}},$$
$$P_3 = \frac{3}{2}a - \frac{c^2}{2(a-1)} + i\frac{c^2(a+9) - 9a^2 + 9a}{6(a-1)^{3/2}}. \tag{20}$$

The above amplitude equation is a stochastic ordinary differential equation, which is also called a stochastic Landau equation. In view of $Re(P_3) > 0$, the Landau equation is supercritical. By using Theorem 5.1 in [33], the stability of Eq. (19) is dependent on the noise tensor δ and the dimensionless distance $b_c - b$. In the following, by setting $b_c - b = \mu\varepsilon^2$ and $A = re^{i\phi}$, it follows from (19) that

$$\frac{dr}{dt} = \mu\varepsilon^2 Re(P_1)r - Re(P_3)r^3$$

$$- \frac{\delta\sqrt{a-1}}{4\pi} \int_0^{2\pi/\omega} \zeta(t) \cos\omega t dt,$$

$$\frac{d\phi}{dt} = \mu\varepsilon^2 Im(P_1) - Im(P_3)r^2$$

$$+ \frac{\delta\sqrt{a-1}}{4\pi} r^{-1} \int_0^{2\pi/\omega} \zeta(t) \sin\omega t dt. \tag{21}$$

In the Landau equation, we have $r \to \varepsilon\sqrt{\frac{Re(P_1)\mu}{Re(P_3)}}$. Thus we have the following two cases.

In case of $\delta \ll \varepsilon^3$, the Eq. (21) is equivalent to

$$\frac{dr}{dt} = \mu\varepsilon^2 Re(P_1)r - Re(P_3)r^3.$$

It means that the additive noise does not affect the dynamic behaviour of the system (1) when present.

In case of $\delta \sim \varepsilon^3$, by setting $\delta_0 = \delta\varepsilon^{-3}$, the long time dynamic behaviour of Eq. (21) is approximately

$$\frac{dr}{dt} = \varepsilon^2\left(\mu Re(P_1)r - \varepsilon\frac{\delta_0\sqrt{a-1}}{4\pi}\int_0^{2\pi/\omega}\zeta(t)\cos\omega t dt\right) - Re(P_3)r^3.$$

Since $\int_0^{2\pi/\omega}\zeta(t)\cos\omega t dt \leq \frac{4}{\omega}$, the solution of the above equation approximates a positive stationary state after a long time, provided that

$$\mu Re(P_1)r > \frac{\delta_0}{\pi}\varepsilon.$$

Substituting $r = \varepsilon\sqrt{\frac{Re(P_1)\mu}{Re(P_3)}}$ into the above equation, we have

$$\delta < \varepsilon^3\frac{\sqrt{a-1}\pi\mu^{\frac{3}{2}}}{\sqrt{12a(a-1) - 4c^2}} := \delta_c. \tag{22}$$

In short: We have obtained a threshold value of the noise tensor, δ_c. When the noise tensor is lower than this value, the stochastic (2) and deterministic (1) systems are equivalent. Therefore, the limiting cycle induced by the Hopf bifurcation sustains in the presence of the additive noise. However, when the noise tensor is higher than this threshold, the two systems can be qualitatively different, and the additive noise can destroy the Hopf bifurcation, leading to unstable limiting cycle.

III.   NUMERICAL SIMULATIONS

In this section we perform numerical simulations of the system (2) by means of a finite difference scheme [34–36], with the help of a Crank-Nicholson scheme for time integration, and a Adams-Bashforth scheme for the nonlinear operator. We consider the system (2) in a fixed spatial domain $[0, L_x] \times [0, L_y]$ ($L_x = 200, L_y = 200$) and solve it on a grid of size 200×200 . Step sizes of space and time are, respectively, $\Delta x = \Delta y = 1$ and $\Delta t = 0.001$. We apply the following parameter values

$$a = 1.1,\ c = 0.1,\ d = 1, \varepsilon^2 = 0.01,$$
$$b = 1 - \varepsilon^2, \delta = \delta_0\varepsilon^3, \tag{23}$$

under which the deterministic system (1) undergoes a Hopf bifurcation at $b = b_c = 1$.

We now explore how the occurence of additive noise in the system (1) will affect the emergence of periodic solutions induced by Hopf bifurcation. To this end, we turn to the amplitude equation (19). Since the equation (9) contains the eigenvalue ρ, in order to obtain the amplitude of system (2), we need to rescale ρ to $(1, (1 - i\sqrt{a-1})/a)^T$. Using the same argument as in

the above section, we derive that $Re(P_1) = \frac{a}{2(a^2+a-1)}$ and $Re(P_3) = \frac{3a^2}{2(a^2+a-1)} - \frac{c^2(2a^2+3a+5)}{6(a-1)(a^2+a-1)}$. Then the modulus of the amplitude satisfies

$$\frac{dr}{dt} = \frac{a\mu\varepsilon^2}{2(a^2 + a - 1)}r$$
$$- \left(\frac{3a^2}{2(a^2 + a - 1)} - \frac{c^2(2a^2 + 3a + 5)}{6(a-1)(a^2 + a - 1)}\right)r^3$$
$$- \frac{\delta\sqrt{a-1}}{4\pi}\int_0^{2\pi/\omega}\zeta(t)\cos\omega t dt. \tag{24}$$

For the given parameters in (23) and the condition (22), we have $\delta_c = 1.74$. We shall see if $\delta_0 < \delta_c$ the additive noise will not affect the emerging periodic solutions. Hence we choose $\delta_0 = 0.5$, alternatively, $\delta = \delta_0\varepsilon^3 = 0.5\varepsilon^3$. Figure 1 shows that the solutions from the amplitude equation predicted by equation (24) and from the system (2) are located at a fixed spatial point. Clearly the amplitude solution agrees qualitatively with the numerical solution during a time scale $(0, O(\varepsilon^{-2})]$ in both the deterministic (left panel) and stochastic (right panel) systems.

However, if $\delta > \delta_c$, we show that the additive noise breaks down the Hopf bifurcation, leading to chaotic dynamics. Figure 2 exhibits the dynamic behaviour of the activator for two cases $\delta_0 < \delta_c$ and $\delta_0 > \delta_c$. Clearly, the solution remains periodic in the former case but becomes chaotic in the other case, which means that additive noise of level lower than δ_c does not affect the Hopf bifurcation (left panels) but will destroy the Hopf bifurcation (right panels) if the level is higher than δ_c.

We now demonstrate two types of spatial patterns (spiral and target waves) that emerge in the stochastic system under suitable initial conditions. The spiral wave is a kind of special travelling wave, which is self-organized at the center of the spatial defect points where the initial densities are the same as equilibrium densities. Since the oscillating amplitude depends on the dimensionless control parameter distance $b_c - b = \mu\varepsilon^2$, we choose $\varepsilon^2 = 0.23$. Figure 3 illustrates the spiral waves under the following initial condition

$$u(x, y)|_{t=0} = u^* - 0.002(x - 0.1y - 90),$$
$$v(x, y)|_{t=0} = v^* - 0.002(y - 100),$$

where there is one defect point at the space location $(100, 100)$. Apparently, one spiral wave emerges around the defect point. During our attempts to generate spiral waves, we find that the time to generate spiral waves depends on the oscillation amplitude. The larger the amplitude, the less time is required to generate spiral waves. We also find that the oscillating frequency is correlated with the width of spiral waves, which increases with parameter a. A similar observation is valid for the target waves (Fig. 4), which emerge under the following initial distribution

$$u(x, y)|_{t=0} = u^* + 10^{-4}e^{-\left((x-100)^2 + (y-100)^2\right)/400},$$

$$v(x,y)|_{t=0} = v^* + 10^{-4} e^{-\left((x-100)^2 + (y-100)^2\right)/400}.$$

IV. CONCLUSION

We have induced additive noise into a reaction-diffusion system to model the effects of a heterogeneous environment. By means of multiscale analysis, we have derived an amplitude equation to describe the oscillatory dynamics of the stochastic system. We found that the impact of additive noise depends on both the dimensionless distance to ε^3 and the noise tensor δ: (1) when $\delta \ll \varepsilon^3$, the additive noise does not affect the dynamic behaviour of the deterministic system, which means that the stochastic system is equivalent to the deterministic counterpart; (2) when $\delta < \varepsilon^3 \frac{\sqrt{a-1}\pi\mu^{\frac{3}{2}}}{\sqrt{12a(a-1)-4c^2}}$, the additive noise alters the oscillatory dynamics quantitatively. Specifically, the oscillatory dynamics in the deterministic system remains periodic but with slightly altered oscillating amplitude in the presence of the additive noise; (3) when $\delta > \varepsilon^3 \frac{\sqrt{a-1}\pi\mu^{\frac{3}{2}}}{\sqrt{12a(a-1)-4c^2}}$, the additive noise alters the oscillatory dynamics qualitatively. The periodic solutions in the deterministic system turn into chaos when the additive noise kicks in.

Our numerical experiments showed that two types of wave patterns (spiral and target) appeared in the stochastic system (2). Moreover, the time required to generate the spiral wave is dependent on both the amplitude and frequency of oscillations that emerge in the stochastic system, and the larger the frequency and the amplitude, the easier for the system to generate spiral waves. In addition, we found the frequency of oscillation decreases the width of spiral waves. Our analytical and numerical results shed light on the understanding of pattern formation in reaction-diffusion systems with additive noise.

APPENDIX

LINEAR STABILITY ANALYSIS

We perform a linear stability analysis for the deterministic system (1). The linear truncated equation of system (1) can be written as $\frac{\partial \mathbf{U}}{\partial t} = L\mathbf{U}$, where $\mathbf{U} = (u,v)^T$ and

$$L = \begin{pmatrix} \Delta + 1 & -a \\ 1 & d\Delta - b_c \end{pmatrix}.$$

Since $\frac{\partial \mathbf{U}}{\partial t} = L\mathbf{U}$ is subject to a periodic boundary condition, we look for a solution in the following form

$$\begin{pmatrix} u \\ v \end{pmatrix} = \sum_k \begin{pmatrix} u^{(k)} \\ v^{(k)} \end{pmatrix} e^{\lambda t} \cos kx. \qquad (A.1)$$

Here λ is the growth rate of the perturbation in time t, and k is the wavenumber. Substituting Eq. (A.1) into the truncated equation, we obtain the following matrix equation

$$\left(\lambda \mathbf{I} - \begin{pmatrix} -k^2 + 1 & -a \\ 1 & -dk^2 - b_c \end{pmatrix} \right) \begin{pmatrix} u^{(k)} \\ v^{(k)} \end{pmatrix} = \begin{pmatrix} 0 \\ 0 \end{pmatrix}.$$

Therefore, we have the dispersion relation

$$\lambda^2 + g(k)\lambda + h(k) = 0, \qquad (A.2)$$

where $g(k) = (1+d)k^2 - 1 + b_c$ and $h(k) = dk^4 + (1-d)k^2 - 1 + a$. It is well-known that a Hopf instability occurs when $g(k) = 0$ and $h(k) > 0$. Thus we can get the critical value of the bifurcation parameter $b = b_c \equiv 1$, which corresponds to the wavenumber $k_c = 0$. The growth rate $\lambda = \pm\sqrt{a-1}i$ gives the frequency $\omega = \sqrt{a-1}$.

[1] A. Turing, Philos. Trans. R. Soc. London, Ser. B **237**, 37 (1952).
[2] V. Castets, E. Dulos, J. Boissonade, and P. De Kepper, Phys. Rev. Lett. **64**, 2953 (1990).
[3] P. De Kepper, V. Castets, E. Dulos, and J. Boissonade, Physica D **49** 161 (1991).
[4] Q. Ouyang and H. L. Swinney, Nature **352**, 610 (1991).
[5] V. Duffet and J. Boissonade, J. Chem. Phys. **96**, 664 (1992).
[6] H. Malchow, Proc. R. Soc. Lond. B **251**, 103 (1993).
[7] P. K. Maini, K. J. Painter, and H. N. P. Chau, Journal of the Chemical Society, Faraday Transactions **93**, 3601 (1997).
[8] H. Malchowa, B. Radtkea, M. Kallachea, A. B. Medvinskyb, D. A. Tikhonovb, and S. V. Petrovskiic, Nonlinear Anal. RWA **1**, 53 (2000).

[9] T. Frisch, S. Rica, P. Coullet, and J. M. Gilli, Phys. Rev. Lett. **72**, 1471 (1994).
[10] L. S. Schulman and P. E. Seiden, Science **233**, 425 (1986).
[11] A. N. Zaikin, A. M. Zhabotinsky, Nature **225**, 535 (1970).
[12] S. Jakubith, H. H. Rotermund, W. Engel, A. von Oertzen, and G. Ertl, Phys. Rev. Lett. **65**, 3013 (1990).
[13] J. Lechleiter, S. Girard, E. Peralta, and D. Clapham, Science **252**, 123 (1991).
[14] J. D. Murray, E. A. Stanley, and D. L. Brown, P. Roy. Soc. B-Biol. Sci. **229**, 111 (1986).
[15] G. Denaro, D. Valenti, A. La Cognata, B. Spagnolo, A. Bonanno, G. Basilone, S. Mazzola, S. W. Zgozi, S. Aronica, and C. Brunet, Ecological Complexity **13**, 21 (2013).
[16] B. Spagnolo, A. Fiasconaro, and D. Valenti, Fluctuation and Noise Letters **3**, L177 (2003).
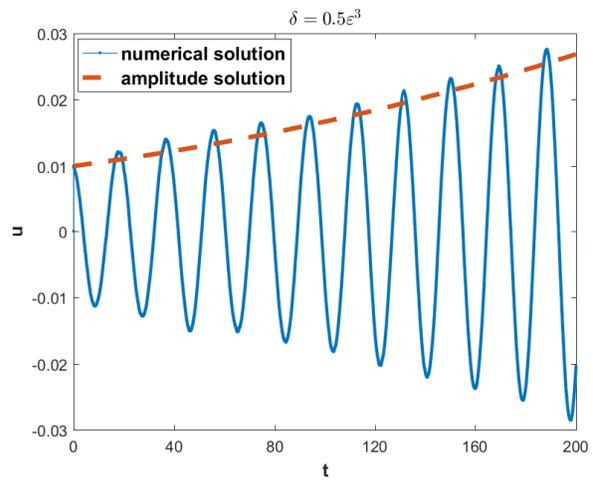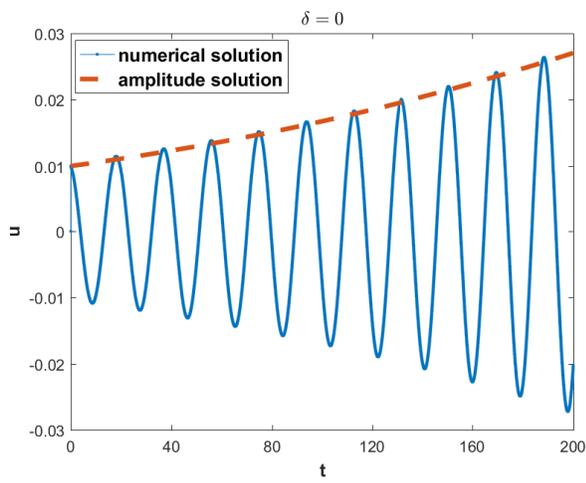
Fig. 1. Solutions to the amplitude equation (dashed line) and to the system(2) (solid line) for two different levels of the noise tensor. Parameters are given in equation (23).

[17] B. Spagnolo, D. Valenti, and A. Fiasconaro, Math. Biosci. Eng. **1**, 185 (2004).

[18] D. Valenti, L. Schimansky-Geier, X. Sailer, and B. Spagnolo, Eur. Phys. J. B **50**, 199 (2006).

[19] D Valenti, A Fiasconaro, and B Spagnolo, Physica A **331**, 477 (2004).

[20] D. Valenti, G. Denaro, A. La Cognata, B. Spagnolo, A. Bonanno, G. Basilone, S. Mazzola, S. Zgozi, and S. Aronica, Acta Phys. Pol. B **43**, 1227 (2012).

[21] A. Zaikin and L. Schimansky-Geier, Phys. Rev. E **58**, 4355 (1998).

[22] J. Garcia-Ojalvo and J. M. Sancho, *Noise in Spatially Extended Systems* (Springer-Verlag, New York, 1999).

[23] G. Agez, M. G. Clerc, E. Louvergneaux, and R. G. Rojas, Phys. Rev. E **87**, 042919 (2013).

[24] M. G. Clerc, C. Falcón, and E. Tirapegui, Phys. Rev. E **74**, 011303 (2006).

[25] D. Blömker, S. Maier-Paape, and G. Schneider, Disc. Contin. Dyn. Syst. Ser. B **1**, 527 (2001).

[26] A. Hutt, A. Longtin, and L. Schimansky-Geier, Phys. Rev. Lett. **98**, 230601 (2007).

[27] A. Hutt, Europhysics Letters **84**, 34003 (2008).

[28] Z. P. Kilpatrick and G. Faye, SIAM Journal on Applied Dynamical Systems **13**, 830 (2014).

[29] C. R. Laing and A. Longtin, Physica D **160**, 149 (2001).

[30] M. Pradas, D. Tseluiko, S. Kalliadasis, D. T. Papageorgiou, and G. A. Pavliotis, Phys. Rev. Lett. **106**, 060602 (2011).

[31] U. Sommer, *Algen, Quallen, Wasserfloh: Die Welt des Planktons* (Springer-Verlag, Berlin, 1996).

[32] H. J. G. Baretta-Bekker, E. K. Duursma, and B. R. Kuipers, *Encyclopedia of Marine Sciences* (Springer-Verlag, Berlin, 1998).

[33] D. Blömker, Stoch. Dynam. **5**, 441 (2005).

[34] X. Zhang, G. Sun, and Z. Jin, Phys. Rev. E **85**, 021924 (2012).

[35] G. Gambino, M. Lombardo, M. Sammartino, and V. Sciacca, Phys. Rev. E **88**, 042925 (2013).

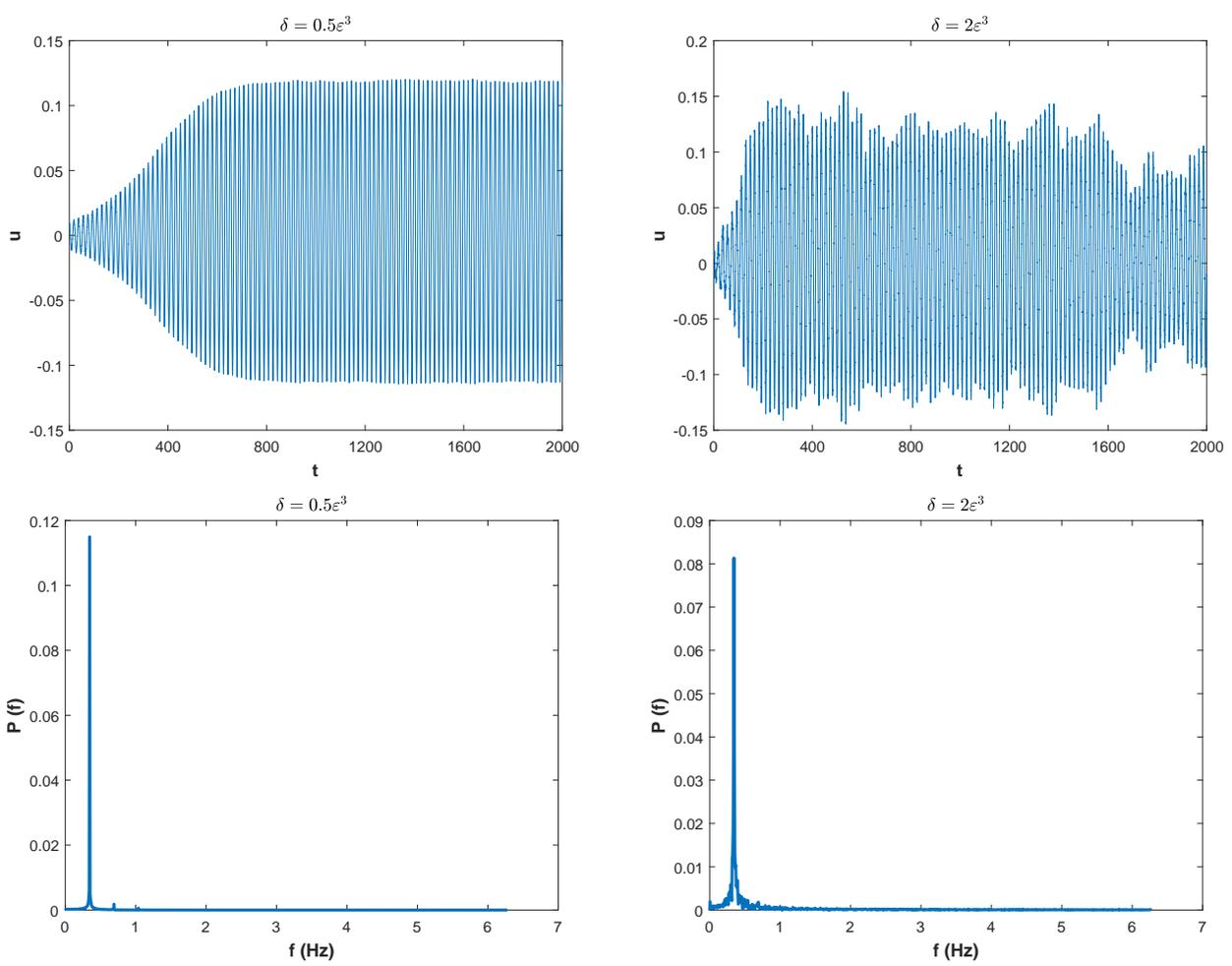[36] C. Tian, L. Lin, and L. Zhang, Appl. Math. Modelling **46**, 423 (2017).

Fig. 2. Time series of the activator density (top panels) at a given spatial location and the associated Fourier spectrum (bottom panels) for two different levels of the additive noise. Parameters are given in equation (23).
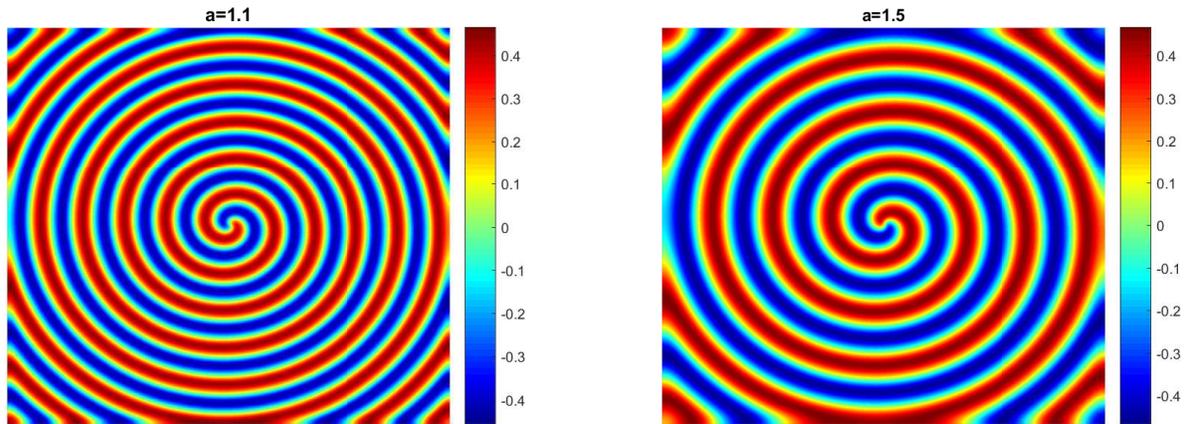

Fig. 3. Snapshot of emerging spatial patterns in the stochastic system (2) at $t = 2000$ for parameter $a = 1.01$(left panel) and $a = 1.5$ (right panel). Here $\varepsilon^2 = 0.23$, $\delta = 0.5\varepsilon^3$. The remaining parameters are given in equation (23).
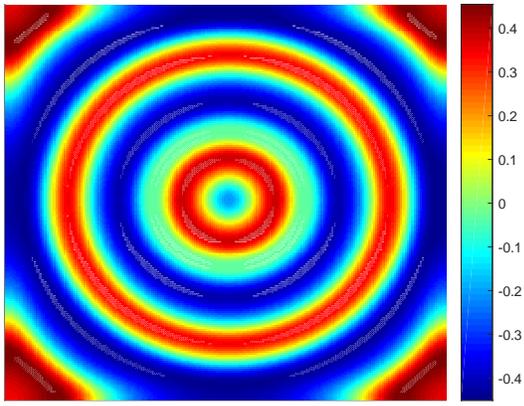
Fig. 4. Snapshot of emerging spatial patterns in the stochastic system (2) at $t = 300$. Here $a = 1.01$, $\varepsilon^2 = 0.23$, $\delta = 0.5\varepsilon^3$. The remaining parameters are given in equation(23).